Kinetic Characterization of the ATPase Activity of the DNA Packaging Enzyme from Bacteriophage λ†

Mary Ann Tomka‡ and Carlos Enrique Catalano*,§

Department of Chemistry and Biochemistry, University of Colorado, Boulder, Colorado 80309, and School of Pharmacy, C238, University of Colorado Health Sciences Center, Denver, Colorado 80262

Received June 10, 1993; Revised Manuscript Received August 27, 1993®

ABSTRACT: Terminases are enzymes common to all of the complex double-stranded DNA viruses and are required for viral assembly. These enzymes function to excise a single viral genome from a concatemeric DNA precursor and package it into a preformed protective protein shell or capsid. ATP hydrolysis by these enzymes has been described and appears to be critical to the packaging process. We have previously characterized the endonuclease activity of purified terminase from bacteriophage λ [Tomka, M. A., & Catalano, C. E. (1993) *J. Biol. Chem. 268*, 3056–3065], and we describe here a kinetic characterization of the ATPase activity of the enzyme. λ terminase possesses a DNA-stimulated ATPase activity and hydrolyzes ATP to ADP and P_i. This activity requires divalent metal and is supported by all of the group IIa metals examined, as well as Mn^{2+}. The reaction is also stimulated by NaCl, GTP, and dGTP. Of note is that neither of the guanosine nucleotides is hydrolyzed by the enzyme, while dATP is hydrolyzed at a rate comparable to that of ATP. Kinetic analysis of the ATPase activity revealed two apparent binding sites for ATP hydrolysis. The high-affinity site ($K_m = 5\ \mu M$) and low-affinity site ($K_m \approx 1.3$ mM) hydrolyze ATP with $k_{cat} = 3$ and 16 min^{-1}, respectively. While the high-affinity site is unaffected by the presence of DNA, ATP hydrolysis at the low-affinity site is stimulated by DNA, which results from both a decrease in the K_m and a concomitant increase in the k_{cat} of the reaction. The implications of these results in the packaging of viral DNA by terminase enzymes are discussed.

We are interested in the mechanisms of assembly of viral precursors into infectious viral particles. Similar mechanisms have been proposed for all of the double-stranded bacteriophages and likely apply to mammalian viruses such as adenovirus and herpes virus (Roizman & Sears, 1991; Black, 1989). Terminases are enzymes common to all of these viruses and function to package a viral genome into a protective protein coat, known as the capsid or head (Feiss, 1986; Murialdo, 1991; Becker & Murialdo, 1990). We are currently investigating the terminase enzyme from bacteriophage λ as a model system for studying viral assembly at the molecular level. This enzyme possesses site-specific endonuclease, helicase, and ATPase activities, all of which work in concert to excise a single viral genome from a concatemeric DNA precursor and package it within a preformed prohead (Murialdo, 1991; Becker & Murialdo, 1990).

The packaging pathway for bacteriophage λ has been described (Murialdo, 1991; Becker & Murialdo, 1990), and it is initiated by the binding of terminase to a DNA sequence known as *cos*[1] (cohesive end site). This sequence represents the junction between the left and right ends of individual (mature) λ genomes in a concatemeric DNA precursor, the preferred substrate for genome packaging. The enzyme introduces staggered nicks at *cos* (endonuclease activity) and separates the nicked, annealed strands (helicase activity), thus forming the first single-stranded "sticky" end of the mature λ genome. This binary enzyme·DNA intermediate (complex I) then captures an empty viral prohead, forming complex II, and the enzyme unidirectionally translocates across the duplex, thus packaging the viral genome into the head. Upon encountering the next downstream *cos* sequence, terminase again nicks the DNA duplex and releases the DNA-filled capsid, which is further processed into a fully infectious viral particle. Packaging is processive, and roughly 3–4 genomes are packaged per DNA binding event (Murialdo, 1991; Becker & Murialdo, 1990).

It has been demonstrated that ATP is required for *in vitro* virus assembly (Becker et al., 1977), and several roles for the nucleotide have been proposed (Murialdo, 1991; Becker & Murialdo, 1990). It is commonly accepted that ATP hydrolysis by λ terminase is required to power unidirectional translocation of the enzyme along the DNA duplex during the packaging process (Black, 1989). ATP hydrolysis also appears to supply the energy required to separate the nicked, annealed strands formed by *cos* cleavage (Higgins et al., 1988). A final, ill-characterized role for ATP centers on fidelity in DNA nicking by the enzyme. In the absence of ATP, *cos* cleavage is slow and error-prone, such that four base single-strand ends are formed rather than the natural 12-base overhang (Higgins et al., 1988). It has been suggested that ATP is required to assemble a catalytically competent multiprotein complex at *cos* to initiate DNA nicking with high fidelity (Murialdo, 1991; Becker & Murialdo, 1990).

We are interested in how the multiple catalytic activities of λ terminase interact to effect packaging of a single viral genome from a concatemeric precursor. Toward this goal, we have previously examined the endonuclease activity of the enzyme (Tomka & Catalano, 1993) and now extend these studies to characterize the biochemical properties of the ATPase activity of the DNA packaging enzyme from bacteriophage λ. The reaction has been optimized with respect to buffer pH, salt, and divalent metal requirements. The effect of other nucleotides on ATP hydrolysis has been examined, as was the capacity of the enzyme to hydrolyze these compounds. Kinetic characterization of the enzyme has

† This work was supported by NSF Grant DMB-9018767.
* Address correspondence to this author.
‡ Department of Chemistry and Biochemistry.
§ School of Pharmacy.
® Abstract published in *Advance ACS Abstracts,* October 15, 1993.
[1] Abbreviations: bp, base pair; *cos*, cohesive end site; IHF, *E. coli* integration host factor; TE, 10 mM Tris-HCl/1 mM EDTA (pH 8.0).

0006-2960/93/0432-11992$04.00/0

revealed that ATP is hydrolyzed at two sites with different affinities for the nucleotide substrate.

EXPERIMENTAL PROCEDURES

Materials. λ DNA, poly(dT), oligo(dT)$_{30}$, pGEM-9Zf, and restriction enzymes were purchased from Promega. The DNA oligonucleotides described in these studies were obtained from Oligos, Etc. Tryptone, yeast extract, and agar were purchased from Difco. Cellulose PEI-F TLC plates were obtained from J. T. Baker. All divalent metals were purchased from Mallinkrodt as dichloride salts. Nucleoside triphosphates, nucleoside diphosphates, and ampicillin were purchased from Sigma Chemical Company. Radionucleotides were obtained from ICN Biochemicals. All other materials were of the highest quality commercially available.

Protein purifications utilized a Pharmacia FPLC system which consisted of two P500 pumps, a GP250-plus controller, a V7 injector, and a Uvicord SII variable-wavelength detector. Radioactivity data were obtained using a Beckman Model LS6000IC scintillation counter. UV–visible absorbance spectra were recorded on a Hewlett-Packard HP8452A diode array spectrophotometer.

Bacterial Strains, Preparation of DNA Substrates, and Protein Purification. AZ1930, an *Escherichia coli* strain which expresses bacteriophage λ terminase (Chow et al., 1987), was a generous gift of H. Murialdo (University of Toronto, Toronto, ON, Canada). A cell line which harbors the plasmid pWP14 (Shinder & Gold, 1988) was obtained from M. Gold (University of Toronto, Toronto, ON, Canada). JM107-[pAFP1] was kindly provided by M. Feiss (University of Iowa, Iowa City, IA), and HN880, an *E. coli* strain which overproduces integration host factor (Nash et al., 1987), was a generous gift of H. Nash (National Institutes of Health, Bethesda, MD).

The plasmids pWP14 and pAFP1 were prepared essentially as described previously (Tomka & Catalano, 1993), except that the DNA was purified by size-exclusion chromatography. Briefly, the crude DNA was applied to a Sephadex G-100 column (2.5 × 20 cm) equilibrated with 20 mM Tris-HCl (pH 8.0), 1 mM EDTA, and 50 mM NaCl buffer, and the DNA was eluted using the same buffer. Column fractions were examined by spotting aliquots on a cellulose PEI-F TLC plate, and the nucleic acids were visualized with a hand-held short-wavelength UV lamp. DNA-containing fractions were pooled, the plasmid was precipitated with isopropyl alcohol, and the pellet was resolubilized in TE (pH 8.0). *Sca*I-linearized pWP14 was prepared as previously described (Tomka & Catalano, 1993). The concentration of the plasmid was determined from the absorbance at 260 nm and a calculated formula weight of 1.99 × 10^6 gm/mol.[2]

A 266-bp *cos*-containing DNA substrate was prepared from pAFP1, a plasmid which contains the entire λ *cos* sequence cloned into M13 (M. Feiss, personal communication). The plasmid was digested with *Eco*RI and *Hin*dIII according to the manufacturer's instructions, and the fragment was purified by 8% PAGE. The concentration of the fragment was determined from the absorbance at 260 nm and a calculated formula weight of 1.7 × 10^5 g/mol.[2]

[2] The concentration of DNA was determined spectrally, assuming 50 μg/mL duplex DNA yields an OD_{260} of 1.0. This was converted to a molar concentration using the indicated formula weight, which was calculated by summation of the formula weights for all of the individual bases in the duplex.

A 30-bp duplex, whose sequence corresponds to the terminase DNA-binding sequence (R-site) (Feiss, 1986; Murialdo, 1991), was obtained from Oligos, Etc. The single-stranded oligonucleotides were purified by denaturing 10% PAGE, and their concentrations were determined spectrally, as previously described (Catalano et al., 1989). Duplexes were formed by mixing equal amounts of single strands, and duplex formation was confirmed by 10% nondenaturing PAGE.

Purification of λ terminase was performed as previously described (Tomka & Catalano, 1993), and integration host factor was purified by the method of Nash et al. (Nash et al., 1987). Both proteins were homogeneous as determined by SDS–PAGE.

ATPase Assays. Unless otherwise indicated, the reaction mixtures (8 μL) contained 50 mM Tris-HCl (pH 9), 12.5 mM $MgCl_2$, 6 mM spermidine, 7 mM β-ME, 1 mM EDTA, 1 mM [α-^{32}P] ATP, and 100 nM λ terminase. Where indicated, DNA (*Sca*I-linearized pWP14) and IHF were added to a final concentration of 100 nM duplex (600 μM total nucleotide) and 100 nM protein, respectively. The reactions were initiated with the addition of magnesium and allowed to proceed for 20 min at 37 °C. Aliquots (4 μL) were removed from the reaction mixture and quenched with the addition of one-half volume of stop buffer (300 mM EDTA and 30 mM each cold ATP and ADP). Aliquots (4 μL) of the quenched reaction mixtures were spotted onto a cellulose PEI-F TLC plate, and the plate was developed with 190 mM sodium phosphate buffer (pH 7.6). The ATP and ADP spots were visualized with a hand-held short-wavelength UV lamp and/or autoradiography, and the extent of the reaction was quantitated by excision of the radiolabeled nucleotides and scintillation counting. Control experiments (ATP hydrolysis time course) using these conditions were performed to ensure that the aliquots were taken within the linear portion of the reaction curve. The kinetic constants for ATP hydrolysis were determined by nonlinear regression analysis of the experimental data using the Igor data analysis program (Wave Metrics, Lake Oswego, OR).

RESULTS

Optimization of the ATPase Assay Conditions. We have previously examined the endonuclease activity of λ terminase and optimized this reaction with respect to buffer pH, salt concentration, and requirement for divalent metals (Tomka & Catalano, 1993). We present here similar studies on the ATPase activity of the enzyme. While it was originally reported that λ terminase was a DNA-*dependent* ATPase (Gold & Becker, 1983), subsequent studies have demonstrated that the purified enzyme possesses significant ATPase activity in the absence of DNA (Becker & Murialdo, 1990). As with the endonuclease activity of the enzyme (Tomka & Catalano, 1993), the ATPase activity exhibited a broad pH optimum which was maximal at pH ≥8.5 (Figure 1A). The activity decreases rapidly above a pH of 9.5, however, and is likely the result of protein denaturation (not shown). Divalent metal was strictly required for both catalytic activities, and while *cos* cleavage was supported only by Mg^{2+} and Mn^{2+} (Tomka & Catalano, 1993), Table I demonstrates that the ATPase activity was less selective and was supported by several of the divalent metals examined. An increase in the Mg^{2+} concentration revealed a sharp increase in ATPase activity between 1 and 1.5 mM, with little concentration effect beyond this point (Figure 1B).

Unlike *cos* cleavage, which was significantly inhibited by concentrations of NaCl as low as 100 mM (Tomka & Catalano,

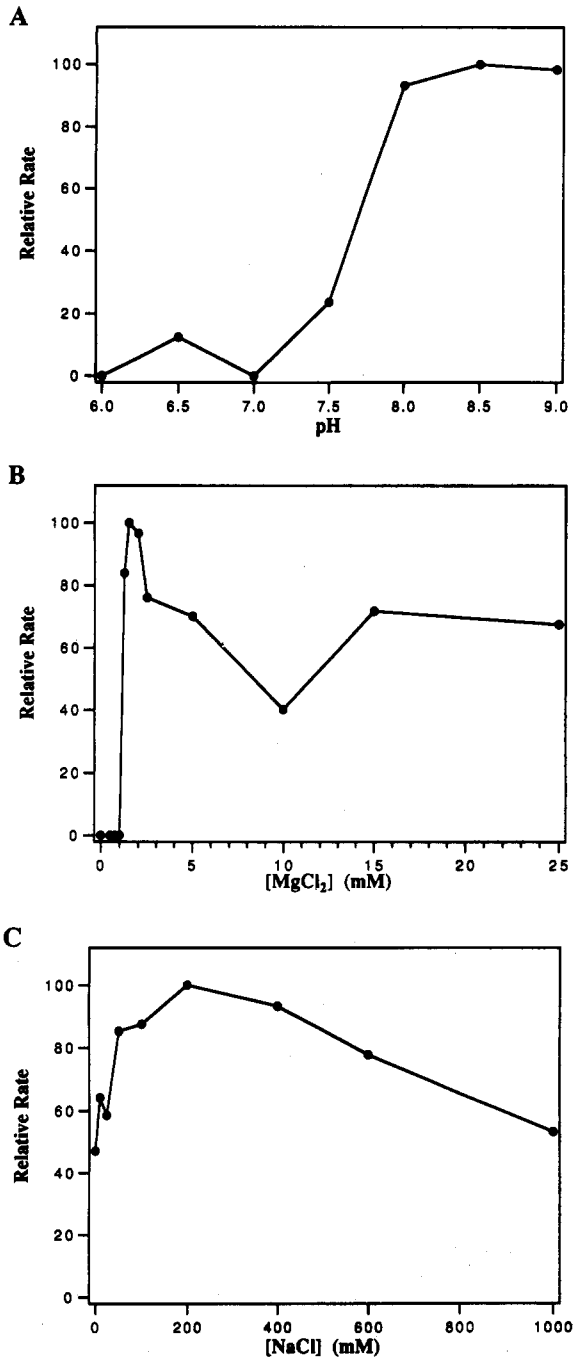

FIGURE 1: Effect of pH, divalent metal, and salt concentration on the ATPase activity of λ terminase. The reaction conditions were as described in the Experimental Procedures, except that (A) the pH of the reaction mixture was adjusted or (B) Mg^{2+} or (C) sodium chloride was added as indicated. The ATPase rates represent the average of experiments done in duplicate.

1993), the ATPase activity of λ terminase was stimulated by salt and was maximal at 200 mM NaCl (Figure 1C). Surprisingly, ATP hydrolysis by the enzyme was substantial even at NaCl concentrations as great as 1 M. Table II demonstrates that DNA also stimulated the ATPase activity of the enzyme by 2–3-fold. DNA-mediated stimulation was saturable and was maximal at a concentration 100 nM pWP14 duplex (not shown). Addition of IHF to the reaction mixture, in the presence or absence of DNA, had no effect on the rate of ATP hydrolysis (not shown). Table II further shows that DNA-mediated stimulation was relatively nonspecific and was observed with both single-stranded and double-stranded DNAs of various lengths. Moreover, the presence of a *cos* sequence

Table I: Divalent Metal Is Required for ATPase Activity[a]

divalent metal	relative ATPase activity
none	ND[b]
Mg^{2+}	100
Ca^{2+}	65
Sr^{2+}	48
Ba^{2+}	44
Mn^{2+}	47
Cd^{2+}	20
Co^{2+}	16
Cu^{2+}	ND
Zn^{2+}	ND

[a] The reaction conditions were as described in the Experimental Procedures, except that the enzyme concentration was increased to 375 nM and the indicated divalent metals were included at a concentration of 10 mM. Elevated enzyme concentrations were used due to the low ATPase activity observed with these metals. The values represent the average of experiments performed in duplicate. 100% activity corresponds to an observed rate of 8.7 min^{-1}. [b] ND denotes $k_{obs} < 0.1$ min^{-1}.

Table II: DNA-Mediated Stimulation of ATPase Activity[a]

DNA substrate	size (bases)	*cos* sequence	single-/double-stranded	relative ATPase activity
none				1
λ DNA (mature)	48502	yes	D	0.6
pWP14	3068	yes	D	2.7
pGEM-9Zf	2925	no	D	2.7
poly(dT)	>2000	no	S	2.1
266_{mer}	266	yes	D	2.0
R-box_{30}	30	no	D	2.7
oligo$(dT)_{30}$	~30	no	S	2.5

[a] The reaction conditions were as described in the Experimental Procedures, except that DNA was added at a concentration of 980 μM (total nucleotide) as indicated in the table. Note that 980 μM pWP14 (total nucleotide) represents a *duplex* concentration of 160 nM. The relative ATPase values listed in the table represent the average of experiments performed in duplicate. A relative activity of 1 corresponds to an observed rate of 8.5 min^{-1}.

Table III: Effect of Sodium Chloride and DNA on ATPase Activity[a]

DNA (nM duplex)	NaCl (mM)	relative ATPase activity
0	0	1
100	0	2.3
0	200	1.6
100	200	1.6

[a] The reaction conditions were as described in the Experimental Procedures, except that sodium chloride and/or DNA (*Sca*I-linearized pWP14) was added as indicated in the table. IHF was included along with DNA at a concentration of 100 nM. The values represent the average of experiments performed in duplicate. A relative activity of 1 corresponds to an observed rate of 11.5 min^{-1}.

was not required for ATPase stimulation. Interestingly, mature λ DNA inhibited the ATPase activity of the enzyme.

We have shown that NaCl stimulated the ATPase activity, but inhibited the endonuclease activity of λ terminase (*vide supra*). We therefore examined the capacity of DNA to stimulate ATP hydrolysis in the presence of NaCl. Table III demonstrates that, while both DNA and NaCl each individually stimulate ATP hydrolysis, additive stimulation in the presence of both compounds was not observed. Rather, the degree of stimulation suggests that, in the presence of salt, DNA had little effect on the capacity of the enzyme to hydrolyze ATP. Gel retardation studies in our laboratory have demonstrated that terminase·DNA complexes were disrupted by salt (not shown), and taken together, these data suggest that the enzyme does not bind DNA in the presence of elevated salt concentrations.

Table IV: Effect of Competing Nucleotides on ATPase Activity[a]

nucleotide added	relative ATPase activity
none	100
ADP	79
PO_4	89
GTP	150
UTP	114
CTP	114
dATP	29
dGTP	143
dTTP	86
dCTP	93

[a] The reaction conditions were as described in the Experimental Procedures, except that the indicated nucleotides were added at a concentration of 5 mM. Note that the [α-^{32}P]ATP substrate was present at a concentration of 1 mM in every case. The values represent the average of experiments performed in duplicate. 100% activity corresponds to an observed rate of 8.5 min^{-1}.

Effect of Competing Nucleotides on ATP Hydrolysis. Table IV shows that the products of ATP hydrolysis (ADP and P_i) had only modest inhibitory effects on the ATPase activity of λ terminase. Moreover, none of the pyrimidine nucleotides examined significantly affected the reaction, even though they were present in 5-fold excess of the radiolabeled ATP substrate. Of note is that, while dATP inhibited the ATPase activity of the enzyme, both ribo- and deoxyguanosine triphosphates *stimulated* ATP hydrolysis (Table IV). Moreover, whereas dATP was hydrolyzed at an observed rate comparable to that of ATP, neither of the guanosine nucleotides was an effective substrate for the NTPase activity of the enzyme when added in place of ATP (data not shown).

Kinetic Analysis of ATP Hydrolysis. An Eadie–Hofstee plot of the observed rate of ATP hydrolysis as a function of ATP concentration was curvilinear and clearly shows the presence of two kinetically distinct ATPase sites (Figure 2A) (Segel, 1975). Several mechanisms may be invoked to explain the multiple catalytic sites, and two simple models were considered initially. Given the tendency of λ terminase to aggregate in solution (Murialdo, 1991; Parris et al., 1988), we first analyzed the data by assuming that the two kinetically identified sites represent ATP hydrolysis by two interconverting enzyme species (e.g., aggregated and nonaggregated):

$$\begin{array}{ccccc} E_1 + ATP & \overset{K_{m1}}{\rightleftharpoons} & E_1{\cdot}ATP & \xrightarrow{k_1} & E_1 + ADP + P_i \\ \Big\| K_{eq} & & & & \\ E_2 + ATP & \overset{K_{m2}}{\rightleftharpoons} & E_2{\cdot}ATP & \xrightarrow{k_2} & E_2 + ADP + P_i \end{array}$$

where E_1 and E_2 represent the two different conformations of the enzyme, each with a distinct affinity for ATP (K_{m1} and K_{m2}) and rate of ATP hydrolysis (k_1 & k_2). The kinetic expression for this model is

$$\frac{k_{obs}}{[E]} = \left[\frac{k_1K_{m2}[ATP] + k_2K_{m1}K_{eq}[ATP]}{K_{m1}K_{m2} + K_{m2}[ATP] + K_{m1}K_{m2}K_{eq} + K_{m1}K_{eq}[ATP]}\right] \quad (1)$$

where [E] is the total enzyme concentration and k_{obs} is the observed rate of ATP hydrolysis at a given concentration of ATP. The data were analyzed using nonlinear regression techniques, and the dashed line displayed in Figure 2B represents the best fit to eq 1. This did not yield a good fit, and no reasonable combination of kinetic constants could be found which accurately described the experimental data. It is unlikely, therefore, that our data represent ATP hydrolysis by two interconverting conformations of the enzyme.

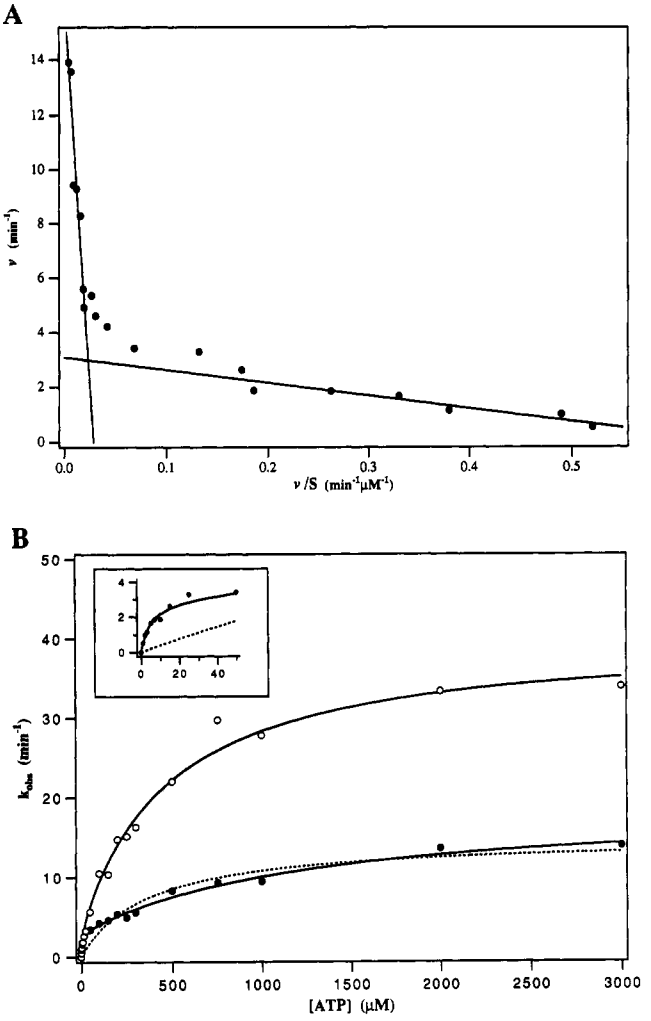

FIGURE 2: Kinetic analysis of the ATPase activity of λ terminase. (A) Eadie–Hofstee plot of the observed rate of ATP hydrolysis as a function of ATP concentration. The reaction conditions were as described in the Experimental Procedures, except that ATP was added as indicated and enzyme was included at 25 nM when low (0–50 μM) ATP concentrations were used. The reaction times were varied between 5 and 20 min to ensure that aliquots were always removed within the linear portion of the reaction curve. Each data point represents the average of experiments done at least in triplicate. Note that the lines represent curves fit to the terminal slopes only and were not used to calculate the kinetic constants presented in the text. (B) A direct plot of the observed rate in the absence (●) and presence (○) of 100 nM DNA (*Sca*I-linearized pWP14). The inset shows an expansion of the data between 0 and 50 μM ATP. The dashed and solid lines represent best fits of the experimental data to eqs 1 and 2, respectively, as described in the text. Note that the addition of DNA to the reaction mixture had little effect on ATP hydrolysis at the low K_m site (not shown). For this reason, the upper curve (○, plus DNA) was generated using the data shown in the inset (no DNA) and that containing DNA and ATP at concentrations between 50 and 3000 μM, as shown.

The data were next analyzed using a model that assumes two independent, noninteracting ATP binding sites within the holoenzyme:

$$E + ATP \overset{K_{m1}}{\rightleftharpoons} E{\cdot}ATP_1 \xrightarrow{k_1} E + ADP + P_i$$

$$E + ATP \overset{K_{m2}}{\rightleftharpoons} E{\cdot}ATP_2 \xrightarrow{k_2} E + ADP + P_i$$

where $E{\cdot}ATP_1$ and $E{\cdot}ATP_2$ represent ATP bound at two

distinct catalytic sites on the protein. The kinetic expression for this model is

$$\frac{k_{obs}}{[E]} = \left[\frac{(k_1[ATP])}{(K_{m1} + [ATP])} + \frac{(k_2[ATP])}{(K_{m2} + [ATP])}\right] \quad (2)$$

where [E] is the total enzyme concentration, k_{obs} is the observed rate of ATP hydrolysis at a given concentration of ATP, and k_1/k_2 and K_{m1}/K_{m2} represent the maximal velocities and Michaelis constants, respectively, for the two binding sites of the holoenzyme. Nonlinear regression analysis of the experimental data using eq 2 yielded the solid line displayed in Figure 2B, and our data are consistent with this simple two-site model.[3]

This analysis also yielded the primary kinetic constants for the reaction: the high-affinity site (K_m = 5 μM) and low-affinity site (K_m = 1267 μM) hydrolyzed ATP with k_{cat} values of 3 and 16 min^{-1}, respectively. Interestingly, DNA had little effect on the activity of the high-affinity site (not shown), and DNA-mediated stimulation of ATPase activity appeared to result primarily from increased catalytic activity at the low-affinity site. Furthermore, analysis of the data presented in Figure 2B revealed that the observed increase in ATP hydrolysis resulted from both a decrease in the K_m (1267 → 470 μM) and a concomitant increase in the k_{cat} (16 → 37 min^{-1}) of the reaction.

DISCUSSION

Our goal is to understand the process of viral assembly at the molecular level. A critical step in the assembly of a virus is packaging of the viral genome within the protective protein capsid. Terminases, the enzymes responsible for this process in double-stranded DNA viruses, possess several catalytic activities which must be coordinated to effect genome packaging. As a first step toward an understanding of viral assembly, we have focused on the endonuclease and ATPase activities of λ terminase. Characterization of λ terminase endonuclease activity has been previously reported (Tomka & Catalano, 1993).

It is of interest to compare the catalytic requirements of the endonuclease and ATPase activities of the enzyme with respect to pH, salt, and divalent metal. Both activities exhibit a broad pH optimum which is maximal at pH ≥8.5 (Tomka & Catalano, 1993; Figure 1A). Sodium chloride at a concentration greater than 100 mM strongly inhibits endonuclease activity (Tomka & Catalano, 1993) but, interestingly, stimulates ATP hydrolysis by the enzyme (Figure 1C). Gel shift experiments have demonstrated that salt disrupts both the binary terminase·DNA complex, as well as the ternary terminase·IHF·DNA complex (M. A. Tomka, unpublished results), and suggest that inhibition of *cos* cleavage by salt is the result of decreased polynucleotide binding to the enzyme. This is consistent with the fact that the DNA-mediated stimulation of ATP hydrolysis by the enzyme appears greatly attenuated in the presence of NaCl (Table III). Taken together, these data further suggest that electrostatic interactions play a major role in DNA recognition by the enzyme. Surprisingly, the ATPase activity of λ terminase is significant at salt concentrations as high as 1 M (Figure 1), and it is of interest that high concentrations of salt (up to 2 M NaCl) similarly stimulate the ATPase activity of recA protein (Pugh & Cox, 1988).

Divalent metal is strictly required for both catalytic activities; however, while there is a gradual increase in endonuclease activity with an increase in the Mg^{2+} concentration between 1 and 25 mM (maximal at 5 mM) (Tomka & Catalano, 1993), ATPase activity increases sharply between 1.0 and 1.5 mM $MgCl_2$ with little concentration effects thereafter (Figure 1B). A similarly sharp increase in catalytic activity at this Mg^{2+} concentration has been noted with yeast DNA polymerase α-complex (Biswas et al., 1993). While our data do not allow us to ascribe a mechanistic interpretation to this observation, it is of note that an increase in the concentration of ATP in the reaction mixture from 1 to 2 mM did not change the Mg^{2+} concentration curve displayed in Figure 1 (data not shown), suggesting that the dramatic increase in activity at 1.5 mM Mg^{2+} was not solely due to the formation of a Mg^{2+}·ATP coordination complex. These data further suggest that, although divalent metal is strictly required for both ATP hydrolysis and *cos* cleavage, its role for each activity may be different. This is punctuated by the fact that, while Mn^{2+} was the only metal that could substitute for Mg^{2+} in DNA cleavage (Tomka & Catalano, 1993), ATPase activity is also supported by all of the group IIa metals examined (Table I).

We note that the rate of ATP hydrolysis by λ terminase under the experimental conditions used in this study is low and only modestly stimulated by DNA (Figure 2B). Moreover, the observed stimulation (2–3-fold) appears to be relatively nonspecific and is observed with a wide range of DNAs (Table II). We previously demonstrated that the endonuclease activity of the enzyme was stoichiometric, rather than catalytic, under similar reaction conditions and was consistent with the formation of complex I, a stable enzyme·DNA intermediate in the packaging pathway (Tomka & Catalano, 1993). We speculate that the slow rate of ATP hydrolysis observed in this study may be associated with the assembly of terminase protomers onto a DNA duplex in an attempt to find a *cos* site to initiate genome packaging. Within this context, it is noteworthy that λ terminase utilizes only ATP and dATP as nucleotide substrates in the hydrolysis reaction. Hydrolysis of ATP or dATP appears to be required for the assembly of a stable transcription complex onto DNA to initiate transcription by RNA polymerase II (Buratowski et al., 1989). This strong nucleotide preference is also found in the majority of helicases examined, including phage T4 Dda protein, *E. coli* helicases I, II, and III, *E. coli* Rep and n′ proteins, as well as uvrAB complex and recBCD enzyme from *E. coli* (Matson & Kaiser-Rogers, 1990). All of these proteins have a strict requirement for divalent metal and K_m's for ATP in the range of 85-550 μM. Interestingly, *E. coli* helicase I and Rep protein also possess high-affinity ATP binding sites, with K_m's of 2 and 21 μM, respectively.

Consistent with this proposed role for ATP hydrolysis in terminase assembly is the observation that, unlike most DNAs examined, mature λ DNA *inhibits* the ATPase activity of the enzyme (Table II). We speculate that mature λ DNA, which already contains the 12-base single-stranded complementary ends formed by terminase cleavage at *cos*, may inhibit ATPase activity by assembling an enzyme·DNA complex (complex I) that no longer requires ATP hydrolysis for stability.

The low rates of ATP hydrolysis observed in our studies conflict with *in vitro* packaging systems that exhibit significant consumption of ATP (Black, 1988, 1989). Terminases utilize the energy of ATP hydrolysis to power translocation across

[3] More complex models involving allosteric regulation and interaction between the two catalytic sites were also considered; however, our data do not allow us to distinguish them kinetically from the simple model presented here.

the DNA duplex during active packaging of the viral genome (Murialdo, 1991; Becker & Murialdo, 1990). It has been demonstrated that *in vitro* packaging by bacteriophage ϕ29 consumes one molecule of ATP for every two base pairs packaged (Guo et al., 1987). Given that the estimated rate of translocation during DNA packaging is 10^4–10^5 min^{-1} (Gope & Serwer, 1983; Shibata et al., 1987), coupling ATP hydrolysis to DNA translocation should rapidly consume ATP. Our assay mixtures lack proheads, however, and translocation presumably does not occur under these experimental conditions. This model predicts that a significant increase in the rate of ATP hydrolysis may be observed upon the addition of viral proheads to *cos*-containing DNA mixtures as the enzyme packages the DNA substrate.

Terminase holoenzyme is composed of two viral-encoded proteins, gpNu1 and gpA, and ATP reactive centers have been identified in the deduced primary amino acid sequences of both polypeptides (Becker & Gold, 1988), suggesting that both subunits might bind and hydrolyze ATP. This has been confirmed by demonstrating that both subunits independently possess ATPase activity (Higgins et al., 1988; Parris et al., 1988). The data presented in Figure 2 demonstrate that terminase holoenzyme possesses two *kinetically* distinct reactive centers. While our data do not allow us to unambiguously assign the physical location of the kinetically identified sites to specific polypeptides, photoaffinity labeling studies using low concentrations of azido-ATP (10 μM) label only gpA to any significant extent (M. Feiss, personal communication). Furthermore, the specific interaction of gpNu1 polypeptide with *cos*-containing DNA has been demonstrated (Shinder & Gold, 1988), and DNA-mediated stimulation of the ATPase activity appears primarily a result of increased activity at the low-affinity site (Figure 2). Taken together, these data suggest (but do not prove) that the high-affinity ATP binding site may reside in gpA, while gpNu1 binds ATP with low affinity.

At present we can only speculate as to the nature of the two ATP binding sites in the function of λ terminase and suggest that one site is involved in terminase assembly onto DNA (*vide supra*) while the second is required to power the translocating complex during active packaging and/or drive the helicase activity of the enzyme. If this model is correct, we would expect that viral proheads and/or a helicase DNA substrate would alter the kinetics of ATP hydrolysis at only one of the two ATPase sites. Experiments investigating the effect of viral proheads on the rate of ATP hydrolysis by λ terminase using purified proheads and DNA substrates of defined sequence are currently underway in our laboratory.

ACKNOWLEDGMENT

We thank Drs. Michael Feiss and Robert Kuchta for helpful discussions and critical review of this manuscript. We are further indebted to Dr. Feiss for informing us of the existence of the high-affinity binding site for ATP and for sharing experimental data prior to publication.

REFERENCES

Becker, A., & Gold, M. (1988) *J. Mol. Biol. 199*, 219–222.
Becker, A., & Murialdo, H. (1990) *J. Bacteriol. 172*, 2819–2824.
Becker, A., Murialdo, H., & Gold, M. (1977) *Virology 78*, 277–290.
Biswas, E. E., Ewing, C. M., & Biswas, S. B. (1993) *Biochemistry 32*, 3020–3026.
Black, L. W. (1988) in *The Bacteriophages* (Calendar, R., Ed.) Vol. 2, Plenum Publishing Corp., New York.
Black, L. W. (1989) *Annu. Rev. Microbiol. 43*, 267–292.
Buratowski, S., Hahn, S., Guarente, L., & Sharp, P. A. (1989) *Cell 56*, 549–561.
Catalano, C. E., Allen, D. J., & Benkovic, S. J. (1989) *Biochemistry 29*, 3612–3621.
Chow, S., Daub, E., & Murialdo, H. (1987) *Gene 60*, 277–289.
Feiss, M. (1986) *Trends Genet. 2*, 100–104.
Gold, M., & Becker, A. (1983) *J. Biol. Chem. 258*, 14619–14625.
Gope, R., & Serwer, P. (1983) *J. Virol. 47*, 96–105.
Guo, P., Peterson, C., & Anderson, D. (1987) *J. Mol. Biol. 197*, 229–236.
Higgins, R. R., Lucko, H. J., & Becker, A. (1988) *Cell 54*, 765–775.
Matson, S. W., & Kaiser-Rogers, K. A. (1990) *Annu. Rev. Biochem. 59*, 289–329.
Murialdo, H. (1991) *Annu. Rev. Biochem. 60*, 125–153.
Nash, H. A., Robertson, C. A., Flamm, E., Weisberg, R. A., & Miller, H. I. (1987) *J. Bacteriol. 169*, 4124–4127.
Parris, W., Davidson, A., Keeler, C. L., & Gold, M. (1988) *J. Biol. Chem. 263*, 8413–8419.
Pugh, B. F., & Cox, M. M. (1988) *J. Biol. Chem. 263*, 76–83.
Roizman, B., & Sears, A. E. (1991) in *Fundamental Virology*, 2nd ed. (Fields, B. N., Knipe, D. M., & Chanock, R. M., Eds.) Vol. 2, Raven Press, New York.
Segel, I. H. (1975) *Enzyme Kinetics*, John Wiley & Sons, New York.
Shibata, H., Fujisawa, H., & Minagawa, T. (1987) *J. Mol. Biol. 196*, 845–851.
Shinder, G., & Gold, M. (1988) *J. Virol. 62*, 387–392.
Tomka, M. A., & Catalano, C. E. (1993) *J. Biol. Chem. 268*, 3056–3065.